

## MANY-BODY METHODS FOR NUCLEAR SYSTEMS AT SUBNUCLEAR DENSITIES

Armen Sedrakian

*Institute for Theoretical Physics, J. W. Goethe-Universität,  
D-60054 Frankfurt am Main, Germany*

*\*E-mail: sedrakian@th.physik.uni-frankfurt.de*

John W. Clark

*Department of Physics, Washington University,  
St. Louis, Missouri 63130, USA*

*\*E-mail: jwc@wuphys.wustl.edu*

This article provides a concise review of selected topics in the many-body physics of low density nuclear systems. The discussion includes the condensation of alpha particles in supernova envelopes, formation of three-body bound states and the BEC-BCS crossover in dilute nuclear matter, and neutrino production in  $S$ -wave paired superfluid neutron matter.

*Keywords:* Nuclear matter; Bose condensations; BCS-BEC crossover; weak interactions.

### 1. Introduction

The physics of matter at subnuclear densities  $\rho \in [10^{11} - 10^{14}] \text{ g cm}^{-3}$  is of great interest for the astrophysics of compact objects. The “hot” stage of evolution of matter, in which temperatures are in the range of tens of MeV, is associated with the dynamics of supernova explosions. Knowledge of the equation of state, composition, and weak-interaction processes are of prime importance for an understanding the mechanism of explosion, the formation of neutrino spectra at the neutrinosphere, and the elemental abundances of the low-density matter in the supernova winds that are prerequisite for the onset of  $r$ -process nucleosynthesis. Days to weeks after the supernova explosion subnuclear matter has become “cold”, with temperatures  $T < 0.1 \text{ MeV}$ . Moreover, the properties of the subnuclear matter forming the crust of a neutron star are of fundamental importance for the entire spectrum of observable manifestations of pulsars, ranging for example from superfluid rotation dynamics to magnetic field evolution to neutrino cooling.

Nuclear matter at subnuclear densities is a strongly correlated system in which the relevant degrees of freedom are well established and the interactions are constrained by experiment. The challenge lies in the many-body treatment of this system where macroscopic quantum phenomena such as Bose-Einstein condensation of

deuterons and alpha particles exist as well as the BCS pairing in neutron matter. Our aim here is to describe some of the many-body methods for dealing with such correlated states of matter. We will pay less attention to the physical setting and implications of the results; the reader concerned with these issues is referred to the original literature cited among the references.

## 2. Bose-Einstein condensation: a lattice Monte-Carlo perspective

In this section we describe an approach to interacting Bose systems which is valid in the vicinity of the critical temperature of Bose-Einstein condensation (BEC). The method was put forward in the context of dilute gases interacting via *repulsive* two-body forces<sup>1,2</sup> and has since been reformulated for a strongly correlated system interacting with *attractive* two-body and repulsive three-body forces.<sup>3</sup> The method has been applied to Bose condensation of alpha particles in infinite matter. (Alternative studies are based on hypernetted-chain summations.<sup>4</sup>) Consider a uniform, non-relativistic system of identical bosons described by the Hamiltonian

$$H = \int d^3x \left[ \frac{\hbar^2}{2m} \nabla \psi^\dagger(\mathbf{x}) \nabla \psi(\mathbf{x}) - \mu |\psi(\mathbf{x})|^2 + g_2 |\psi(\mathbf{x})|^4 + g_3 |\psi(\mathbf{x})|^6 \right],$$

where  $m$  is the alpha-particle mass,  $\mu$  is the chemical potential, and  $\psi$  is the boson field. Below, we shall implement lattice regularization. The theory defined by Eq. (1) can be mapped onto an effective scalar field theory within the finite-temperature Matsubara formalism. Consider the fields  $\psi$  and  $\psi^\dagger$  as periodic functions of the imaginary time  $\tau \in [-\beta, \beta]$ , where  $\beta = 1/T$  is the inverse temperature. Next, decompose the fields into discrete Fourier series

$$\psi(\mathbf{x}, \omega_\nu) = \sum_{\nu=-\infty}^{\infty} e^{i\omega_\nu \tau} \psi(\mathbf{x}, \tau) = \psi_0(\mathbf{x}) + \sum_{\nu=-\infty, \nu \neq 0}^{\infty} e^{i\omega_\nu \tau} \psi(\mathbf{x}, \tau), \quad (1)$$

where the Fourier frequencies  $\omega_\nu$  are the bosonic Matsubara modes  $\omega_\nu = 2\pi i\nu T$  (with  $\nu$  taking integer values). The Matsubara Green's function is given by  $G^M(\omega_\nu, \mathbf{x}) = [i\omega_\nu - (2m)^{-1}\nabla^2 + \mu]^{-1}$ . Here the chemical potential may include any contribution from the momentum- and energy-independent part of the self-energy; we also assume that any momentum and energy dependent parts are absorbed in the mass and the wave-function renormalizations, respectively. Since  $\mu \rightarrow 0$  near  $T_c$ , the characteristic scales of spatial variations of the Green's function with non-zero Matsubara frequencies are  $l = (2m\omega_\nu)^{-1/2}$ , which are of the order of the thermal wave-length  $\lambda = (2\pi/mT)^{1/2}$ . The contribution of the non-zero Matsubara modes to the sum in Eq. (1) will be neglected since we are interested in scales  $L \gg l$ , which are characterized only by the zero-frequency modes. In terms of new real scalar fields  $\phi_1$  and  $\phi_2$  defined via the relations  $\psi_0 = \eta(\phi_1 + i\phi_2)$  and  $\psi_0^\dagger = \eta(\phi_1 - i\phi_2)$ , where  $\eta = \sqrt{m/\hbar^2\beta}$ , the continuum action of the theory is given by

$$S(\phi) = \int d^3x \left\{ \frac{1}{2} \sum_{\nu} [\partial_\nu \phi(\mathbf{x})]^2 + \frac{r}{2} \phi(\mathbf{x})^2 - \frac{u}{4!} [\phi(\mathbf{x})^2]^2 + \frac{w}{6!} [\phi(\mathbf{x})^2]^3 \right\}, \quad (2)$$

where  $\phi^2 = \phi_1^2 + \phi_2^2$ ,  $r = -2\beta\mu\eta^2$ ,  $u = 4!\beta g_2\eta^4$  and  $w = 6!\beta g_3\eta^6$ . The action (2) describes a classical  $O(2)$  symmetric scalar  $\phi^6$  field theory in three spatial dimensions (3D). The positive sextic interaction guarantees that the energy is bound from below, which would not otherwise be the case because of the negative sign of the quartic term describing the attractive two-body interactions. The characteristic length scale of the theory is set by the parameter  $u$ , which has the dimension of inverse length; the dimensionless parameter of the lattice theory is  $ua_L$ , where  $a_L$  is the lattice spacing. The thermodynamic functions of the model are obtained from the partition function

$$Z = \int [d\phi(\mathbf{x})] \exp[-S(\phi)]. \quad (3)$$

For example, the expectation value of the particle number density is given by  $n_\alpha = \langle \psi^* \psi \rangle = (\beta V)^{-1} \partial \ln Z / \partial \mu$ , where  $V$  is the volume. The continuum theory is now discretized on a lattice by replacing the integrations over spatial coordinates by a summation over lattice sites. The discretized version of the continuum action (2) is

$$S_L(\phi) = \sum_i \left\{ -2\kappa \sum_\nu \phi_L(\mathbf{x}) \phi_L(\mathbf{x} + a_L \hat{\nu}) \phi_L(\mathbf{x})^2 + \lambda [1 + \phi_L(\mathbf{x})^2]^2 + \zeta [\phi_L(\mathbf{x})^2]^3 \right\},$$

the  $\nu$  summation being carried out over unit vectors in three spatial directions (nearest neighbor summation). The hopping parameter  $\kappa$  and the two- and three-body coupling constants  $\lambda$  and  $\zeta$  are related to the parameters of the continuum action through  $a_L^2 r = (1 - 2\lambda)/\kappa - 6$ ,  $\lambda = a_L \kappa^2 u/6$ , and  $\zeta = w \kappa^3/90$ . The lattice and continuum fields are related by  $\phi_L(\mathbf{x}) = (2\kappa/a_L)^{1/2} \phi(\mathbf{x})$ . The components of the spatial vector  $x_\nu$  are discretized at integral multiples of the lattice spacing  $a_L$ :  $x_\mu = 0, a_L, \dots, (L_\nu - 1)a_L$ . For a simple cubic lattice in 3D with periodic boundary conditions imposed on the field variable, one has  $\phi_L(x + a_L L) = \phi_L(x)$  (N.B. for a box of length  $L$  there are  $L^3$  (real) variables within the volume  $(La_L)^3$ ).

In Ref. 3, the field configurations on the lattice were evolved using a combination of the heatbath and local Metropolis algorithms, executing  $10^5 - 10^6$  equilibration sweeps for lattices sizes from  $8^3$  to  $64^3$ . Once the field values on the lattice were determined, these were transformed into their counterparts in the continuum theory to obtain the statistical average value  $\langle H \rangle$  of the Hamiltonian, i.e., the grand canonical (thermodynamical) potential  $\Omega$  as a function of density. The critical temperature  $T_c$  for Bose-Einstein condensation can be obtained from the simulations.<sup>3</sup> In practice one obtains the density  $n(T)$ , rather than  $T(n)$  directly, at constant fugacity  $z \rightarrow 1$ . Working at small fugacity  $\log z = -0.1$ , the density of the system at constant small chemical potential can be computed and the associated temperature is then identified with  $T_c$ .

### 3. From pair condensation to three-body bound states

The few-body bound states are of interest in the ‘‘hot’’ stage of compact stars to the extent that they can provide a very efficient source of opacity for neutrinos propa-

gating through matter. This situation can be compared to that of radiative transfer in ordinary stars, where the photoabsorption on the weakly-bound negative ion of hydrogen ( $\text{H}^-$ ) largely determines the opacity. If the system is isospin-symmetric, the pairing occurs in the  ${}^3S_1 - {}^3D_1$  partial-wave channel. There is a two-body bound state in this channel in free space – the deuteron; hence the BCS to BEC crossover arises in this new context.<sup>5–7</sup> Following up on the conjecture of Nozières and Schmitt-Rink,<sup>5</sup> one may attempt to describe this crossover within mean-field BCS theory. The central numerical problem then reduces to solution of the gap equation

$$\Delta_l(p) = - \int \frac{dp' p'^2}{(2\pi)^2} \sum_{l'=0,2} V_{ll'}^{3SD1}(p, p') \frac{\Delta_{l'}(p')}{\sqrt{E(p')^2 + D(p')^2}} [1 - 2f(E(p'))], \quad (4)$$

where  $D^2(k) \equiv (3/8\pi)[\Delta_0^2(k) + \Delta_2^2(k)]$  is the angle-averaged neutron-proton gap function,  $V^{3SD1}(p, p')$  is the interaction in the  ${}^3S_1 - {}^3D_1$  channel,  $E(p)$  is the quasi-particle spectrum, and  $f$  is the Fermi distribution function. The chemical potential is determined self-consistently from the gap equation (4) and the expression for the density.

We now outline an algorithm for numerical solution of the gap equation, which can be applied to arbitrary potentials that are attractive at large separations.<sup>8</sup> The method is effective in dealing with the hard core (short-range repulsion) in nuclear potentials and could be useful for other systems featuring short-range repulsive interactions. The starting point is the gap equation with an ultraviolet momentum cutoff  $\Lambda \ll \Lambda_P$ , where  $\Lambda_P$  is of the order of the natural (soft) cutoff of the potential. Successive iterations, which generate approximant  $\Delta_i$  to the gap function from approximant  $\Delta^{(i-1)}$  ( $i = 1, 2, \dots$ ), are determined from

$$\Delta^{(i)}(p, \Lambda) = \int^\Lambda \frac{dp' p'^2}{(2\pi)3} V^{3SD1}(p, p') \frac{\Delta^{(i-1)}(p', \Lambda)}{\sqrt{E(p')^2 + D^{(i-1)}(p', \Lambda)^2}} [1 - 2f(E(p))]. \quad (5)$$

The process is initialized by first solving Eq. (4) for  $D(p_F)$ , where  $p_F$  is the Fermi momentum, assuming the gap function to be a constant. The initial approximant for the momentum-dependent gap function is then taken as  $\Delta^{(i=0)}(p) = V(p_F, p)D(p_F)$ . Two iteration loops are implemented at given chemical potential. An internal loop operates at fixed  $\Lambda$  and solves the gap equation (5) iteratively for  $i = 1, 2, \dots$ . An external loop increments the cutoff  $\Lambda$  until  $d\Delta(p, \Lambda)/d\Lambda \approx 0$ . The finite range of the potential guarantees that the external loop converges once the entire momentum range spanned by the potential is covered. Thus, choosing the starting  $\Lambda$  small enough, we execute the internal loop by inserting  $\Delta^{(i-1)}(p)$  in the right-hand side of Eq. (5) to obtain a new  $\Delta_i(p)$  on the left-hand side, which in turn is re-inserted in the right-hand side. This procedure converges rapidly to a momentum-dependent solution for the gap equation for  $\Delta(p, \Lambda_j)\theta(\Lambda_j - p)$ , where  $\theta$  is the step function and the integer  $j$  counts the iterations in the external loop.

For the next iteration, the cutoff is incremented to  $\Lambda_j = \Lambda_{j-1} + \delta\Lambda$ , where  $\delta\Lambda \ll \Lambda_j$ , and the internal loop is iterated until convergence is reached. The two-

loop procedure is continued until  $\Lambda_j > \Lambda_P$ , after which the iteration is stopped, a final result for  $\Delta(p)$  independent of the cutoff having been achieved. Once this process is complete, the chemical potential must be updated via the equation for the density. Accordingly, a third loop of iterations seeks convergence between the the output gap function and the chemical potential, such that the starting density is reproduced.

The BCS-BEC crossover<sup>5</sup> in nuclear systems has been studied as a function of density and asymmetry in the population of isospin states (proton-neutron asymmetry). A number of interesting features are revealed.<sup>7,9</sup> In the extreme low-density limit, the chemical potential changes its sign and tends to  $-1.1$  MeV, half the deuteron binding energy. Thus, twice the chemical potential plays the role of the eigenvalue in the Schrödinger equation for two-body bound states in this, the BEC limit. The pair function is very broad in this low-density regime, indicating that the deuterons are well localized in space; conversely it is peaked in the BCS limit at high density where the Cooper pairs are correlated over large distances. In the case of asymmetric systems, the density distribution of the minority particles (protons) has a zero-occupation (blocking) region that is localized around their Fermi-surface. Upon crossover to the BEC side, the blocking region becomes wider and moves toward lower momenta. Eventually there is a topological change in the Fermi surface: the states are occupied starting at some finite momentum and are empty below that point. The Nozières–Schmitt-Rink conjecture<sup>5</sup> of a smooth crossover from the BCS to the BEC limit does not hold in general for asymmetric systems; instead, phases with broken space symmetries intervene within a certain range of population asymmetries (see Ref. 9 and references therein).

The three-body bound states can be computed from the three-body scattering matrix, which is written as  $\mathcal{T} = \mathcal{T}^{(1)} + \mathcal{T}^{(2)} + \mathcal{T}^{(3)}$ , with components defined (using operator notation for compactness) as

$$\mathcal{T}^{(k)} = \mathcal{T}_{ij} + \mathcal{T}_{ij} \frac{Q_3}{\Omega - \epsilon_1 - \epsilon_2 - \epsilon_3 + i\eta} (\mathcal{T}^{(i)} + \mathcal{T}^{(j)}). \quad (6)$$

These are nonsingular type II Fredholm integral equations; the operator  $Q_3$  in momentum representation is given by  $Q_3(\mathbf{k}_1, \mathbf{k}_2, \mathbf{k}_3) = [1 - f(\mathbf{k}_1)][1 - f(\mathbf{k}_2)][1 - f(\mathbf{k}_3)] - f(\mathbf{k}_1)f(\mathbf{k}_2)f(\mathbf{k}_3)$ ; and  $\epsilon_i(\mathbf{k}_i)$  are the quasiparticle spectra. The momentum space for the three-body problem is conveniently spanned by the Jacobi four-momenta  $K = k_i + k_j + k_k$ ,  $p_{ij} = (k_i - k_j)/2$ , and  $q_k = (k_i + k_j)/3 - 2k_k/3$ . The  $\mathcal{T}_{ij}$ -matrices are essentially the two-body scattering amplitudes, embedded in the Hilbert space of three-body states. In the momentum representation they are determined from

$$\langle p|T(\omega)|p' \rangle = \langle p|V|p' \rangle + \int \frac{dp'' p''^2}{4\pi^2} \langle p'|V|p'' \rangle \frac{Q_2(p, q)}{\omega - \epsilon_+(q, p) - \epsilon_-(q, p) + i\eta} \langle p''|T(\omega)|p' \rangle, \quad (7)$$

where  $Q_2(q, p) = \langle 1 - f(\mathbf{q}/2 + \mathbf{p}) - f(\mathbf{q}/2 - \mathbf{p}) \rangle$  and  $\epsilon_{\pm}(q, p) = \langle \epsilon(\mathbf{q}/2 \pm \mathbf{p}) \rangle$  are averaged over the angle between the vectors  $\mathbf{q}$  and  $\mathbf{p}$ . Compared to the free-space problem, the three-body equations in the background medium now include two-

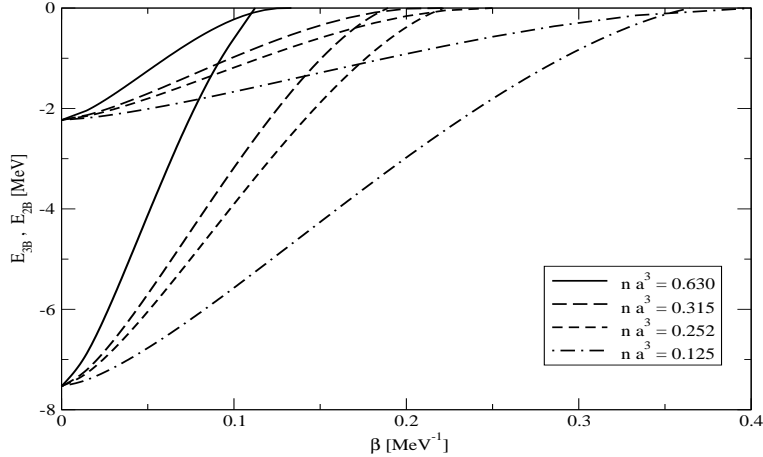


Fig. 1. Dependence of the two-body ( $E_d$ ) and three-body ( $E_t$ ) binding energies on inverse temperature, for fixed values of the ratio  $f = n_0/n$ , where  $n$  is the baryon density and  $n_0 = 0.16 \text{ fm}^{-3}$  is saturation density of nuclear matter. For asymptotically large temperature,  $E_d(\infty) = -2.23 \text{ MeV}$  and  $E_t(\infty) = -7.53 \text{ MeV}$ . The ratio  $E_t(\beta)/E_d(\beta)$  is a universal constant independent of temperature.<sup>8</sup>

and three-body propagators that account for (i) the suppression of the phase-space available for scattering in intermediate two-body states, encoded in the functions  $Q_2$ , (ii) the phase-space occupation for the intermediate three-body states, encoded in the function  $Q_3$ , and (iii) renormalization of the single-particle energies  $\epsilon(p)$ . For small temperatures the quantum degeneracy is large and the first two factors significantly reduce the binding energy of a three-body bound state; at a critical temperature  $T_{c3}$  corresponding to  $E_t(\beta) = 0$ , the bound state enters the continuum.

This behavior is illustrated in Fig. 1, which shows the temperature dependence of the two- and three-body bound-state energies in dilute nuclear matter for several values of the density of the environment. In analogy to the behavior of the in-medium three-body bound state, the binding energy of the two-body bound state enters the continuum at a critical temperature  $T_{c2}$ , corresponding to the condition  $E_d(\beta) = 0$ . Our solutions exhibit a remarkable feature: the ratio  $\eta = E_t(\beta)/E_d(\beta)$  is a constant *independent of temperature*. For the chosen potentials, the asymptotic free-space values of the binding energies are  $E_t(0) = -7.53 \text{ MeV}$  and  $E_d(0) = -2.23 \text{ MeV}$ ; hence  $\eta = 3.38$ . An alternative definition of the critical temperature for trimer extinction is  $E_t(\beta'_{3c}) = E_d(\beta)$ . This definition takes into account the break-up channel  $t \rightarrow d + n$  of the three-body bound state into the two-body bound state  $d$  and a nucleon  $n$ . The difference between the two definitions is numerically insignificant.

Fig. 2 depicts the normalized three-body bound-state wave function for three representative temperatures, as a function of the Jacobi momenta  $p$  and  $q$ . As the temperature drops, the wave function becomes increasingly localized around

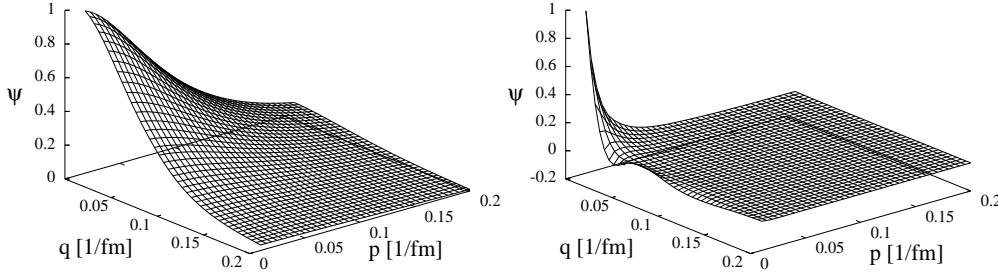


Fig. 2. Wave function of the three-body bound state as a function of the Jacobi momenta  $p$  and  $q$  defined in the text, for  $f = n_0/n = 60$  and temperatures  $T = 60$  (left panel) and  $6.6$  MeV (right panel).

the origin in momentum space. Correspondingly, the radius of the bound state increases in  $r$ -space, eventually tending to infinity at the transition. The wave-function oscillates near the transition temperature (right panel of Fig. 2). This oscillatory behavior is a precursor of the transition to the continuum, which in the absence of a trimer-trimer interaction is characterized by plane-wave states.

#### 4. The weak interaction in cold subnuclear matter

Non-nucleonic channels of cooling that operate in the crusts of neutron stars are electron neutrino bremsstrahlung off nuclei and plasmon decay:<sup>10</sup>  $e + (A, Z) \rightarrow e + (A, Z) + \nu + \bar{\nu}$  and plasmon  $\rightarrow +\nu + \bar{\nu}$ . Above the critical temperature  $T_c$  for neutron superfluidity, the neutrons that occupy continuum states (i.e., those not bound in clusters) emit neutrinos of all flavors  $f$  via the bremsstrahlung process<sup>11</sup>  $n + n \rightarrow n + n + \nu_f + \bar{\nu}_f$ . At  $T \leq T_c$  the latter process is suppressed exponentially by  $\exp(-2\Delta/T)$ , where  $\Delta$  is the gap in the quasiparticle spectrum. The superfluid nature of the matter allows for a neutrino-generating reaction (known as pair-breaking and recombination), whose rate scales like  $\Delta^7$  and thus is specific to the superfluid (i.e., vanishes as  $\Delta \rightarrow 0$ ). The rate of the process is given by the polarization tensor of superfluid matter.<sup>12</sup>

A systematic diagrammatic method to compute the reaction rates is based on the kinetic equation for neutrino transport, formulated in terms of real-time Green's functions.<sup>13</sup> The corresponding Boltzmann equation is

$$[\partial_t + \partial_q \omega_\nu(\mathbf{q}) \partial_x] f_\nu(\mathbf{q}, x) \int_0^\infty \frac{dq_0}{2\pi} \text{Tr} [\Omega^<(q, x) S_0^>(q, x) - \Omega^>(q, x) S_0^<(q, x)],$$

where  $q \equiv (q_0, \mathbf{q})$  is the four momentum,  $S_0^{>,<}(q, x)$  are the neutrino propagators, and  $\Omega^{>,<}(q, x)$  are their self-energies. In second Born approximation with respect to the weak vertices  $\Gamma_{Lq_1}^\mu$ , the latter are given in terms of the polarization tensor(s)

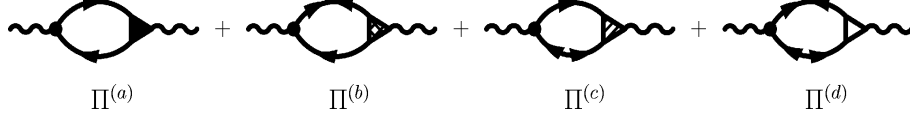


Fig. 3. The sum of polarization tensors that contribute to the neutrino emission rate. The contributions from  $\Pi^{(b)}(q)$  and  $\Pi^{(c)}(q)$  vanish at the one-loop approximation.

$\Pi_{\mu\lambda}^{>,<}(q_1, x)$  of ambient matter as

$$-i\Omega^{>,<}(q, x) = \int \frac{d^4q_1}{(2\pi)^4} \frac{d^4q_2}{(2\pi)^4} (2\pi)^4 \delta^4(q - q_2 - q_1) i\Gamma_{Lq_1}^\mu iS_0^<(q_2, x) i\Gamma_{Lq_1}^{\dagger\lambda} i\Pi_{\mu\lambda}^{>,<}(q_1, x), \quad (8)$$

The “greater” and “lesser” signs refer to the ordering of two-point functions along the Schwinger contour in the standard way.

It is the total loss of energy in neutrinos per unit time and unit volume, i.e., the emissivity, that is of interest for the astrophysics of compact stars. This quantity is obtained by integrating the first moment of Boltzmann equation. For the bremsstrahlung of neutrinos and anti-neutrinos of given flavor it is expressed as

$$\epsilon_{\nu\bar{\nu}} = -\frac{G^2}{4} \sum_{q_1, q_2} \int d^4q \delta(q_1 + q_2 - q) q_0 g(q_0) \Lambda^{\mu\zeta}(q_1, q_2) \text{Im} \Pi_{\mu\zeta}(q), \quad (9)$$

where  $G$  is the weak coupling constant,  $q$  is the four-momentum transfer,  $g(q_0) = [\exp(q_0/T) - 1]^{-1}$  is the Bose distribution function,  $\Pi_{\mu\zeta}(q)$  is the retarded polarization tensor, and  $\Lambda^{\mu\lambda}(q_1, q_2) = \text{Tr}[\gamma^\mu(1 - \gamma_5) \not{q}_1 \gamma^\nu(1 - \gamma_5) \not{q}_2]$ . Sums over the neutrino momenta  $q_{1,2}$  indicate integration over the invariant phase-space volume. The central problem of the theory is to compute the polarization tensor of the cold subnuclear matter. Initially, calculations of the polarization tensor within the superfluid phase were carried out at the one-loop approximation. This treatment was recently shown to be inadequate for the  $S$ -wave superfluid in neutron-star crusts.<sup>14</sup>

A many-body framework that is consistent with the sum rules for the polarization tensor, in particular with the  $f$  sum rule

$$\lim_{\mathbf{q} \rightarrow 0} \int d\omega \omega \text{Im} \Pi^V(\mathbf{q}, \omega) = 0, \quad (10)$$

is provided by the random-phase resummation of the particle-hole diagrams in the superfluid matter. Because of the Nambu-Gorkov extension of the number of possible propagators in the superfluid phase, which now include both normal ( $G$ ) and anomalous ( $F$ ) ones, at least three topologically different vertices are involved, which obey (schematically) the following equations

$$\hat{\Gamma}_1 = \Gamma_0 + v(G\Gamma_1G + \hat{F}\Gamma_3G + G\Gamma_2\hat{F} + \hat{F}\Gamma_4\hat{F}), \quad (11)$$

$$\hat{\Gamma}_2 = v(G\Gamma_2G^\dagger + \hat{F}\Gamma_4G^\dagger + G\Gamma_1\hat{F} + \hat{F}\Gamma_3\hat{F}), \quad (12)$$

$$\hat{\Gamma}_3 = v(G^\dagger\Gamma_3G + \hat{F}\Gamma_1G + G^\dagger\Gamma_4\hat{F} + \hat{F}\Gamma_2\hat{F}), \quad (13)$$



$k_F$ [fm $^{-1}$ ]	$m^*/m$	$\Delta$ [MeV]	$T_c$ [MeV]	$R(0.5)$	$R(0.8)$	$R(0.9)$
0.8	0.97	3.15	1.78	0.014	1.0	6.5
1.6	0.84	0.57	0.38	0.022	1.0	7.4

*Note:* Quoted are the wave number of neutrons, their effective mass, the gap and critical temperature, and the ratio  $R$  as a function of reduced temperature  $T/T_c$ .

$v$  being the scalar interaction in the particle-hole channel. The fourth integral equation for the vertex  $\Gamma_4$  follows upon interchanging particle and hole propagators in Eq. (11). The full polarization tensor is the sum of the contributions shown in Fig. 3. It can be expressed through “rotated” polarization functions  $\mathcal{A}$ ,  $\mathcal{B}$ , and  $\mathcal{C}$  as

$$\Pi^V(q) = \frac{\mathcal{A}(q)\mathcal{C}(q) + \mathcal{B}(q)2}{\mathcal{C}(q) - v^V[\mathcal{A}(q)\mathcal{C}(q) + \mathcal{B}(q)2]} \quad (14)$$

with  $\mathcal{A} = 2\Delta^2 I_0(q) - \Delta^2 \xi_q I_A(q)$ ,  $\mathcal{B} = -\omega \Delta I_0(q)$ , and  $\mathcal{C}(q) = -(\omega^2/2) I_0(q) + \xi_q I_C(q)$ , where  $\xi_q = q^2/2m$  is the nucleon recoil. (The integrals  $I_0$ ,  $I_C$ , and  $I_A$  can be found in Ref. 14.) It is now manifest that  $\Pi^V(q) = 0$  when  $q = 0$ . Thus, the leading order contribution to the polarization tensor appears at  $O(q^2)$  and is linear in  $\xi_q$ . Since the neutrinos are thermal, with energies  $\omega \sim |\mathbf{q}| \sim T$ , the polarization tensor is suppressed by a factor  $T/m$ , which is of order  $5 \times 10^{-3}$ .

The emissivity of the pair-breaking process can be compared to that of the modified bremsstrahlung (MB) process  $n + n \rightarrow n + n + \nu + \bar{\nu}$ , which is suppressed by roughly a factor  $\exp(-2\Delta/T)$  in the superfluid phase. Thus, the ratio of the neutrino loss rate through MB to that from the pair-breaking process, as computed by Friman and Maxwell,<sup>11</sup> is

$$R = \frac{2460\pi^4}{14175} \kappa \left(\frac{g_A}{c_V}\right)^2 \left(\frac{T}{\Delta}\right)^2 \left(\frac{m_n^*}{m_\pi}\right)^4 \frac{F}{I_0} \exp\left(-\frac{2\Delta}{T}\right), \quad I_0 = \int_{\frac{2\Delta}{T}}^{\infty} dx x^5 f\left(\frac{x}{2}\right)^2,$$

where  $g_A$  and  $c_V$  are the weak axial and vector coupling constants,  $m_n^*$  and  $m_\pi$  are the neutron and pion masses, and  $F \simeq 0.6$  (defined in Ref. 11). The factor  $\kappa = 0.2$  accounts for the correction to the one-pion-exchange rate due to the full resummation of ladder series in neutron matter. The pair-breaking process dominates the MB process for temperatures below  $0.8T_c$ , where it is most efficient. This is illustrated in the table above. The comparison made here should be taken with caution, since the exponential suppression of the MB rate is not accurate (within a factor of a few) at temperatures close to the critical temperature. Nevertheless, one may safely conclude that the vector-current pair-breaking process is competitive with the modified pair-bremsstrahlung process in the relevant temperature domain  $T/T_c \in [0.2 - 1]$ .

## 5. Closing remarks

Subnuclear matter at finite temperatures offers a fascinating arena for the development of many-body theory. Since the interactions involved are well constrained by experiment, the entire complexity arises from the many-body correlations. As shown

in the examples chosen, subnuclear matter may exhibit a range of salient many-body phenomena, such as Bose-Einstein condensation of alpha particles, BEC-BCS crossover in the deuteron channel, many-body extinction of bound states with increasing degeneracy, and non-trivial and quantitatively important modifications of the weak interaction rates due to many-body effects.

### Acknowledgements

We thank H. Mütter and P. Schuck for their contribution to the research described in this article. We are grateful to the organizers of RPMBT14 for their impressive efforts and dedication in arranging a most successful conference.

### References

1. G. Baym, J.-P. Blaizot, and J. Zinn-Justin, *Europhys. Lett.* **49** (2), 150 (2000).
2. J. Zinn-Justin, arXiv:hep-ph/0005272.
3. A. Sedrakian, H. Mütter and P. Schuck, *Nucl. Phys. A* **766**, 97-106 (2006).
4. M. T. Johnson and J. W. Clark, *Kinam* **3**, 3 (1980) also made available at this URL <http://wuphys.wustl.edu/Fac/facDisplay.php?name=Clark.txt>
5. P. Nozières and S. Schmitt-Rink, *J. Low Temp. Phys.* **59**, 195 (1985).
6. T. Alm, B. L. Friman, G. Röpke and H. Schulz, *Nucl. Phys. A* **551**, 45 (1993).
7. U. Lombardo, P. Nozières, P. Schuck, H. J. Schulze and A. Sedrakian, *Phys. Rev. C* **64**, 064314 (2001) [arXiv:nucl-th/0109024].
8. A. Sedrakian and J. W. Clark, *Phys. Rev. C* **73**, 035803 (2006).
9. A. Sedrakian and J. W. Clark, in "Pairing in Fermionic Systems: Basic Concepts and Modern Applications", eds. A. Sedrakian, J. W. Clark, and M. Alford, World Scientific, pp. 145-175, [arXiv:nucl-th/0607028].
10. G. G. Festa and M. A. Ruderman, *Phys. Rev.* **122**, 1317 (1969); J. B. Adams, M. A. Ruderman, and C. H. Woo, *Phys. Rev.* **129**, 1383 (1963).
11. O. V. Maxwell and B. L. Friman, *Astrophys. J.* **232**, 541 (1979); D. N. Voskresensky and A. V. Senatorov, *Sov. J. Nucl. Phys.* **45**, 411 (1987) [*Yad. Fiz.* **45**, 657 (1987)]; A. Sedrakian and A. E. L. Dieperink, *Phys. Lett. B* **463**; E. van Dalen, A. E. L. Dieperink, and J. A. Tjon, *Phys. Rev. C* **67**, 580 (2003).
12. E. G. Flowers, M. Ruderman, and P. G. Sutherland, *Astrophys. J.* **205**, 541 (1976); D. N. Voskresensky and A. V. Senatorov, *Sov. J. Nucl. Phys.* **45**, 411 (1987) [*Yad. Fiz.* **45**, 657 (1987)]. A. B. Migdal, E. E. Saperstein, M. A. Troitsky, and D. N. Voskresensky, *Phys. Rep.* **192**, 179 (1990);
13. A. Sedrakian and A. E. L. Dieperink, *Phys. Rev. D* **62**, 083002 (2000); A. Sedrakian, arXiv:astro-ph/0701017; see also D. N. Voskresensky and A. V. Senatorov in ref. 12.
14. A. Sedrakian, H. Mütter and P. Schuck, arXiv:astro-ph/0611676; see also L. B. Leinson and A. Perez, *Phys. Lett. B* **638**, 114 (2006) [arXiv:astro-ph/0606651].